PCCP

Accepted Manuscript

ROYAL SOCIETY OF CHEMISTRY

www.rsc.org/pccp

Journal Name

RSCPublishing

ARTICLE

Hydrogen-bonding interactions of uric acid complexes with water/melamine revealed by mid-infrared spectroscopy

Hiroyuki Saigusa,* Daisuke Nakamura and Shu-hei Urashima‡

Cite this: DOI: 10.1039/xoxxoooooox

Received ooth January 2012,
Accepted ooth January 2012

DOI: 10.1039/xoxxoooooox

www.rsc.org/

Hydrogen (H)-bonding interactions of uric acid (UA) with water have been investigated via IR–UV double resonance measurements in the mid-IR region. Comparison of the present results with those obtained previously in the near-IR region enables us to examine microscopic hydration effects specific to the H-bonding acceptor sites of UA. It is shown that hydration to the C8O site promotes mode coupling of this stretch with the C2O stretch. The occurrence of this coupling is manifested in the IR intensity pattern; transition associated with their in-phase contribution C8O + C2O is significantly suppressed while corresponding out-of-phase contribution gives rise to a strong peak. We have also measured the mid-IR spectra of the 1:1 complex formed between UA and melamine (MEL) and carried out its structural analysis using the spectroscopic signature of H-bonding derived from the result of the monohydrated cluster. It is shown that the complex possesses triple H-bonding structure with the C2O acceptor site of UA H-bonded with MEL. Furthermore, the technique of IR-depleted UV spectroscopy is employed in order to ascertain whether other structural isomers are present in the probe UV spectra.

Introduction

The structures of most biomolecules are determined by the corrective influence of many weak interactions. Among them, H-bonding interactions of biomolecules with water are particularly important in the stabilization of specific conformations that can exhibit biological functions.[1] Therefore, identification of both donor (D) and acceptor (A) sites involved in H-bonding is essential for molecular understanding of the relation between the structural features and proper functioning.[2]

Chart 1 Structures of uric acid (UA) and melamine (MEL).

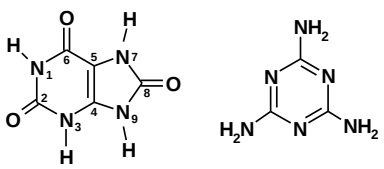

UA MEL

UA (Chart 1), the final product of purine catabolism, is only sparingly soluble in water, and thus excreted in the urine as a paste of the crystals.[3] Since it possesses four NH and three CO sites in its tri-keto form (Chart 1), it is suitable for the investigation of H-bonding preference with water. In our previous work,[4] the technique of laser-desorption and supersonic-jet was utilized to generate monohydrated clusters of UA in the gas phase, and their structural analyses were performed by IR spectroscopy in the NH and OH stretching frequency regions in combination with theoretical calculations. Two structurally different monohydrates were found and assigned to the two most stable isomers, both with UA in its triketo form. In one isomer, water is bound to the N3H site (denoted W23) while in the other, hydration occurs to the N9H site (denoted W89). Details of hydration preference were discussed on the basis of the observed frequency shift associated with the NH stretching vibrations.

Multiple H-bonding interactions of UA with MEL (Chart 1) were also studied[5] in relation to the serious food safety incident that urinary stones are accumulated in infants after ingesting melamine (MEL)-contaminated formula.[6-8] Analysis of urinary stones by high-performance liquid chromatography–mass spectrometry (HPLC−MS) showed that most stones are composed of UA and MEL at a molar ratio of 1:1 to 2:1.[9] On this basis, it was suggested that a 1:1 complex (denoted UA−MEL) stabilized by triple H-bonds is responsible for the stone formation.[7,10] Motivated by these clinical studies, we carried out structural analysis on the corresponding complex formed in the gas phase. A single isomer was detected, and its

IR spectrum recorded in the near-IR region only showed that in this complex the two donor sites (N3H and N9H) of UA are occupied by H-bonding with MEL. Nevertheless, it was not possible to identify the acceptor site of the triple H-bonds (either C2O or C8O site).

In the present work, IR−UV double resonance spectroscopic measurements on the monohydrated cluster of UA and UA−MEL complex are extended to the mid-IR region[11-20] to elucidate how hydration to a specific CO site of UA affects the frequency and intensity of this stretching mode and others. It is shown that hydration to the C8O position of UA enables for coupling of this mode with C2O stretch mode. The occurrence of this mode coupling is manifested in the IR intensity pattern of these stretch transitions. By using this spectroscopic signature of H-bonding, the observed UA−MEL complex is unambiguously identified as the calculated most stable structure, in which the C2O site of UA is H-bonded to the amino hydrogen of MEL.

Methods

Gas-phase isolation of UA and production of its hydrates and complexes with MEL was performed by the laser desorption technique, as described in detail elsewhere.[21] The powder sample of UA or a mixture of UA and MEL (1:1 in molar ratio), each added with a graphite matrix (10%), was used to prepare a sample pellet. It was placed in a stainless holder and irradiated by the second harmonics of a neodymium-doped yttrium aluminum garnet (Nd:YAG) laser. The plume of desorbed molecules was entrained into a supersonic expansion of argon (5 atm) in order to facilitate complex formation. For producing hydrated clusters, the carrier gas was passed through a reservoir containing water.

Infrared Spectroscopy

Hydrated cluster of UA and 1:1 complex of UA−MEL formed by this method were ionized through resonant two-photon ionization (R2PI) using a frequency tunable UV laser, and analyzed by a TOF mass spectrometer.[22-24] Mass-selected UV spectra were recorded by probing ion signal at a particular mass channel while scanning UV laser frequency. IR spectra were recorded in the mid-IR (1500−1800 cm^{-1}) by the IR−UV double-resonance scheme, but not normalized with respect to the IR laser fluence (1–2 mJ/pulse, focused with a cylindrical CaF_2 lens of f=300 mm). The IR radiation was produced by difference frequency generation of the signal and idler outputs of an optical parametric oscillator and amplifier (OPO/OPA) system (LaserVision) using a $AgGaSe_2$ crystal. The rotation-vibration lines of water vapor[25] were used for frequency calibration. The probe UV light (~0.1 mJ/pulse, focused with a cylindrical lens of f=500 mm) was the frequency-doubled output of a YAG-pumped dye laser. The UV laser was operated at a repetition rate of 10Hz, and delayed by 100 ns with respect to the IR laser at 5 Hz. The alternate UV signals measured with IR laser turned on (I_{on}) and off (I_{off}) were fed into a boxcar integrator, and displayed as depletion yields defined by log (I_{off} / I_{on}).

Additional IR-UV double resonance measurements were performed by fixing IR laser to a prominent vibrational transition of a particular isomer and scanning UV laser. The resulting IR-depleted UV spectra enable us to examine if spectral features of other isomers are embedded in the UV spectra.[4,26]

Computational Methods

All calculations were performed using the Gaussian 09 quantum code package.[27] Geometries of monohydrated cluster of UA and 1:1 complex UA–MEL were optimized at the second-order Møller–Plesset's perturbation (MP2) method with the 6-311++G(d,p) basis set. Thereafter, single-point calculations were carried out for the lower-energy structures at the Coupled-Cluster including all Single and Double excitations (CCSD) level with the same basis set, to improve the accuracy of their energetic ordering. Vibrational frequency calculations were performed for the optimized geometries using the Density Functional Theory (DFT)'s B3LYP hybrid functional (a parametrized combination of Becke's exchange functional, the Lee, Yang, and Parr correlation functional, and exact exchange functional) with the 6-311++G(d,p) basis set. The calculated frequencies were scaled by a factor of 0.982 to account for the observed frequencies of C6O stretches of monomer.

Results and discussion

Low-energy isomers of monohydrate of UA and UA–MEL complex

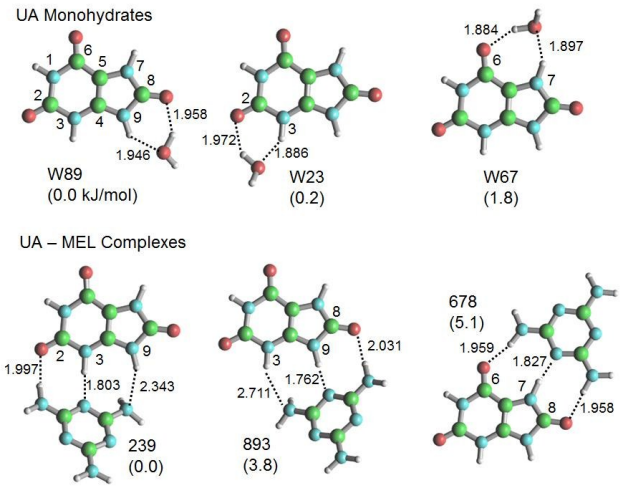

Fig. 1 The three lowest-energy isomers calculated for UA monohydrate (top) and UA−MEL complex (bottom). Stabilization energy (in kJ/mol) with respect to the most stable isomer is indicated in parentheses. Formation of H-bonds is indicated by the dotted line with its distance in angstrom.

Low-energy structures of the monohydrate of UA and UA−MEL complex calculated at the MP2 level of theory with the 6-311++G(d,p) basis set are shown in Fig. 1. In the case of the monohydrate, two isomers W89 and W23 are nearly isoenergetic and lower in energy than isomer W67.[4,28,29] Two lowest-energy structures of UA-MEL are found to be structures 239 and 893 of ADD(UA) – DAA(MEL) type,[5] in which two H-bonding sites (23 and 89) correspond to those occupied in the monohydrates W23 and W89, respectively. In both structures, two molecular pairs are stabilized by triple H-bonding and significantly folded each other. On the contrary, structure 678 is of ADA(UA) – DAD(MEL) type, which is nearly planar and higher in energy due to significant pyramidalization of the two amino groups of MEL.[30]

Monohydrated clusters of UA

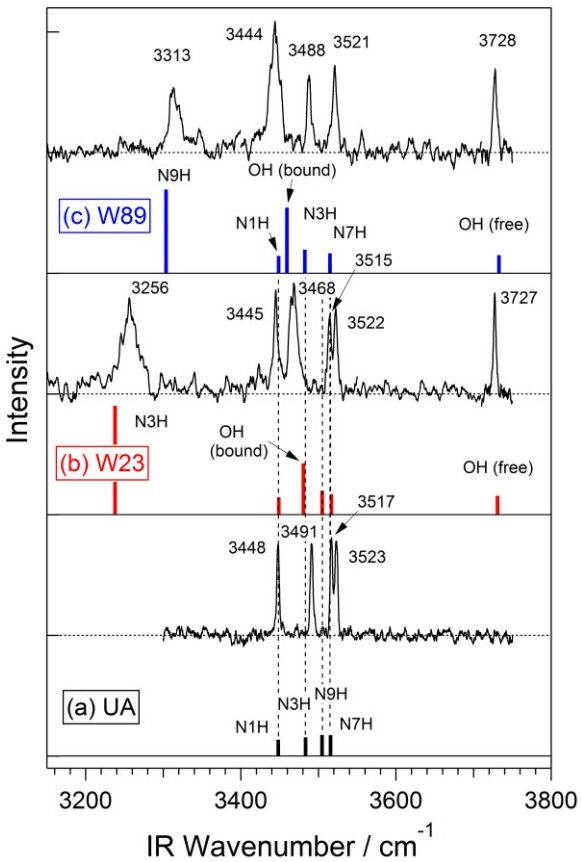

Fig. 2 IR spectra of (a) UA monomer, and monohydrated clusters (b) W23 and (c) W89, recorded in the near-IR region. The UV probe frequencies used to record the IR spectra are 34051 cm^{-1} for W89 and 34071 cm^{-1} for W23, which are indicated by the arrows in Figs. 4(a) and 4(b), respectively. Vibrational spectra calculated at the B3LYP/6-311++G(d,p) level (scaled by a factor of 0.958, ref. 4) are also shown. The vertical, dotted lines are used for guiding the calculated NH stretch transitions. Vibrational frequencies appear to be different from those in the previous report (ref. 4) as a result of frequency calibration.

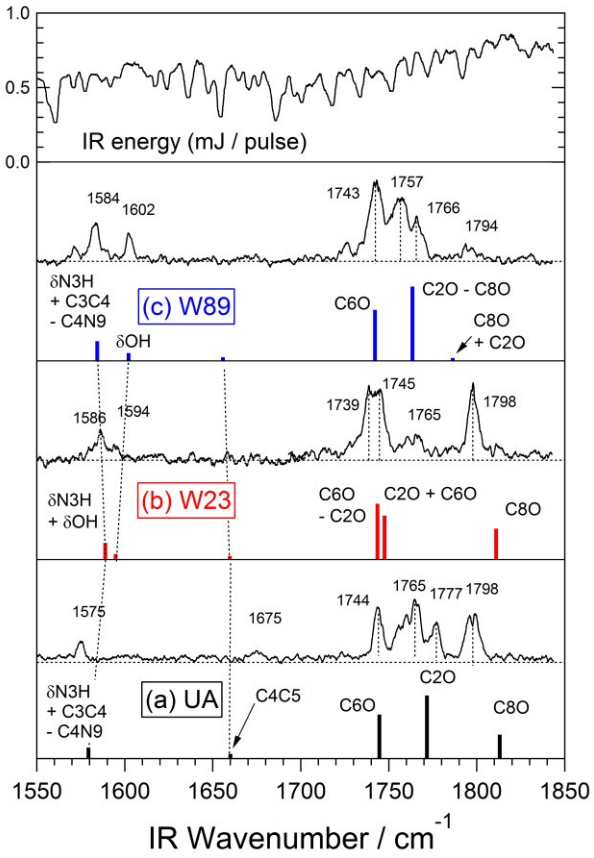

Fig. 3 Mid-IR spectra recorded for (a) UA monomer, and two monohydrates (b) W23 and (c) W89. The vertical lines in the experimental spectra correspond to positions of the indicated frequencies. Vibrational spectra calculated at the B3LYP/6-311++G(d,p) level (scaled by a factor of 0.982) are also shown. Energy curve of the mid-IR laser is shown in top panel. The UV frequencies used to record the respective IR spectra are the same as those in Fig. 2.

We have previously shown that the UV spectrum recorded by probing R2PI signal at the mass channel of monohydrate ion consists of many sharp peaks that can be assigned to either isomer W89 or W23.[4] This enables us to record the IR spectra of respective isomers. In order to make comparison with the mid-IR spectra of these monohydrates discussed later, the corresponding near-IR spectra recorded with better signal-to-noise ratio are displayed in Fig. 2, together with that of UA. The monomer spectrum in Fig. 2(a) reveals four prominent bands corresponding to free NH stretching vibrations. In contrast, the spectrum of W23 in Fig. 2(b) reveals no peak corresponding to free N3H stretching vibration (3491 cm^{-1} in UA monomer), which is consistent with this H-bonding structure. In the top spectrum recorded for isomer W89, transition due to free N9H transition of UA (3517 cm^{-1}) is absent, which indicates that this site is hydrated. Instead, a broad red-shifted band is observed at 3313 cm^{-1} and assigned to that of bound N9H stretch vibration. The transition associated with bound OH stretch of water is observed at 3444 cm^{-1} in W89 and 3468 cm^{-1} in W23 while respective free OH stretching transitions occur at 3728 and 3727 cm^{-1}.

The corresponding mid-IR spectra are shown in Fig. 3, in comparison with the calculated and scaled spectra (with a scaling factor of 0.982). The monomer spectrum in Fig. 3(a) shows three strong bands at 1744, 1765, and 1798 cm^{-1}, which are assignable to C6O, C2O, and C8O stretching vibrations, respectively, in comparison with the calculated spectra. The potential energy distribution analysis[31] provided by DFT frequency calculation indicates that C2O and C8O 'internal' modes of UA are somewhat coupled each other, and thus the bands at 1765 and 1798 cm^{-1} are ascribed more precisely to their out-of-phase [C2O(65%) – C8O(14%)] and in-phase [C8O(62%) + C2O(12%)] contributions, respectively.[32] The 1744 cm^{-1} band is assigned to the stretching vibration predominantly localized on the C6O mode. An additional peak is observed at 1777 cm^{-1}, which is likely to occur due to mode coupling (or Fermi-type resonance) between one of CO stretching vibrations and a combination of low-frequency vibrations. In addition, some peaks are accompanied by noticeable dips [e.g., on the top of the 1798 cm^{-1} peak in Fig. 3(a)], which are due to absorption of the IR laser beam by water vapour (top panel). The strong peak located at 1575 cm^{-1} is assigned to mixed modes with substantial contributions from two stretches N3C4 and C4N9, and N3H bend (δN3H).[32]

The mid-IR spectrum obtained for isomer W23 [Fig. 3(b)] shows a strong band at 1798 cm^{-1}, which is predominantly due to C8O mode. As a result of H-bonding to the C2O site, its stretching frequency is expected to decrease, allowing for

coupling with C6O stretch mode. Therefore, the doublet structure observed at 1745 and 1739 cm^{-1} can be associated with the in-phase and out-of-phase contributions of the two stretch modes C2O ± C6O. This behaviour is in striking contrast to the case of NH stretching vibrations shown in Fig. 2 where frequency reduction induced by hydration are much larger and thus mode coupling with other NH stretches is unlikely to occur. A weak shoulder observed at 1594 cm^{-1} corresponds well to the calculated frequency of the bending vibration of water (δOH).

Our normal mode analysis for isomer W89 indicates that H-bonding at the C8O site mediates vibrational coupling of this mode with C2O mode. Accordingly, the calculated two transitions in Fig. 3(c) are better described by the in-phase and out-of-phase combinations of the two internal modes with nearly equal contributions. In this case, the C8O and C2O stretch motions are almost in the opposite directions, and thus the IR activity of their symmetric combination (C8O + C2O) is substantially suppressed as manifested in Fig. 3(c). This in turn suggests that the strong band at 1757 cm^{-1} can be assigned to the out-of-phase (antisymmetric) combination of the two stretch modes (C2O – C8O). Furthermore, the strong band at 1743 cm^{-1} agrees in frequency well with pure C6O stretching vibration of monomer, which led us to assign this band to the corresponding transition of isomer W89. A weak shoulder observed at 1766 cm^{-1} is tentatively assigned to a combination band with a low-frequency vibration.

Having observed that the mid-IR spectra of isomers W23 and W89 differ each other, the technique of IR-depleted UV spectroscopy is carried out to examine whether spectral features of other isomers are embedded in the UV spectra.[4,26] In this method, IR laser of a higher pulse energy (2mJ/pulse) is tuned to a specific transition of a given isomer. As a result of depopulation in the vibrational ground state, its contribution to the UV signal is effectively suppressed. Thus, we expect that the resulting UV spectrum is composed of isomers which are not subject to depopulation. Conversely, UV spectrum of the isomer that is depleted with this IR irradiation can be obtained by recording the difference between the R2PI signals with the IR laser turned on and off.

Fig. 4 shows the UV spectra of the monohydrated clusters recorded with IR laser turned on (I_{on}) at the prominent CO stretching bands displayed in Fig. 3. The spectra with IR laser turned off (I_{off}), and their difference spectra ($I_{on} – I_{off}$) are also shown. The spectra shown in Fig. 4(a) are obtained with IR laser tuned to C2O – C8O transition of isomer W89 at 1757 cm^{-1} shown in Fig. 3(c). Upon this IR irradiation, ground-state population of isomer W89 is expected to be washed out while isomer W23 survives. The observed IR-depleted spectrum I_{on} is found to match well that obtained with IR laser fixed at the free N3H transition[4] [the 3488 cm^{-1} peak of isomer W89 in Fig. 2(c)]. Since the N3H position of isomer W23 is H-bonded with water, IR irradiation at free N3H transition allows us to record the UV spectra of isomers having no free N3H site (i.e., isomer W23).

If IR laser is tuned to the strong transition of W23 appearing at 1798 cm^{-1} in Fig. 3(b), then we expect the depleted spectrum I_{on} to display spectral features associated with isomer W89. In fact, the observed I_{on} spectrum shown in Fig. 4(b) resembles the difference spectrum $I_{on} – I_{off}$ in Fig. 4(a), and assigned predominantly to that of W89. Moreover, it is noted that the I_{on} spectrum agrees with the corresponding spectrum recorded with IR depletion at free N9H transition.[4]

The UV spectra shown in Fig. 4(c) are obtained upon IR irradiation at the 1743 cm^{-1} band, which is assigned to C6O stretching transition of W89. Since this transition lies in close proximity to the broad features assigned to the two transitions of W23 (1739 and 1745 cm^{-1}), we expect that both isomers are subject to depletion by this irradiation. Indeed, it can be seen in Fig. 4(c) that the UV signal I_{on} is nearly suppressed. This support the presumption that the UV spectrum I_{off} is composed of spectral features of the two isomers and contribution of other isomers such as the next stable isomer W67 in Fig. 1 is negligible in this UV energy region. The vibrational frequency of C6O mode calculated for isomer W67 is substantially lower than this depletion frequency as a result of hydration to this site, as shown in Fig. S1 (ESI †). The absence of W67 in this UV energy region has been interpreted by a theoretical calculation.[29] The result predicts that the excitation energy of this isomer having an H-bond at the C6O site is substantially lower than in the other isomers, thus resulting in insufficient one-color R2PI signal.

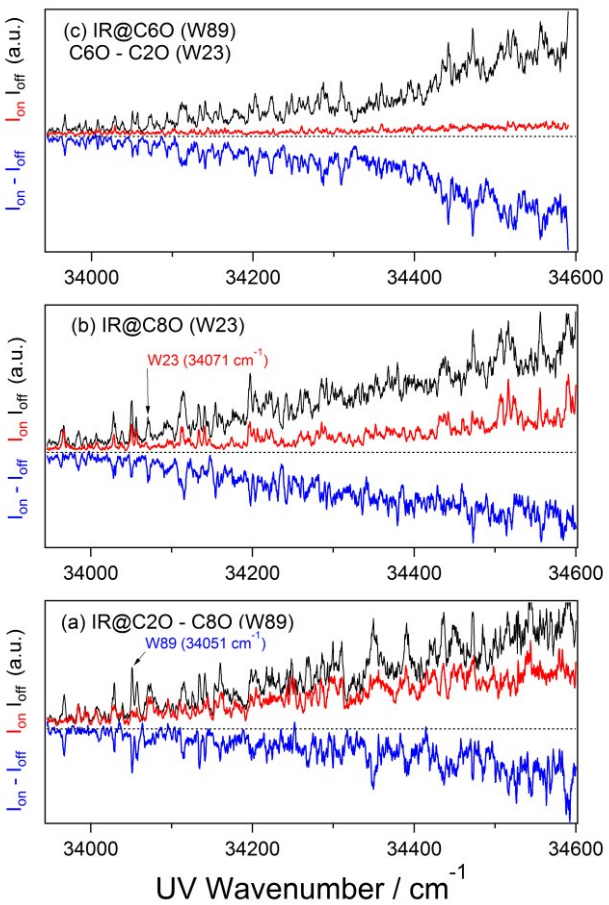

Fig. 4 IR-depleted UV spectra (I_{on}, red) and difference UV spectra ($I_{on} – I_{off}$, blue) recorded for the monohydrated clusters with IR laser tuned to the prominent transitions in Fig. 3: (a) C2O – C8O of isomer W89 at 1757 cm^{-1}, (b) C8O of W23 at 1798 cm^{-1}, and (c) C6O of W89 and C6O – C2O of W23 at 1743 cm^{-1}. UV spectra recorded with IR laser turned off (I_{off}) are shown in black. The arrows shown in parts (a) and (b) indicate the UV peaks of isomers W89 and W23 used to record the respective IR spectra given in Figs. 2 and 3.

UA–MEL complex

In our previous report,[5] we showed that the UV spectrum of the UA–MEL complex located in the region of >33500 cm^{-1} appears to be broad with no well-resolved peaks. It was also found that the IR spectra obtained by the IR-UV double resonance method are basically independent of the probe UV frequency. Based on these observations, it was suggested that only one conformer is responsible for the observed UV spectrum.

For ease of discussion, the experimental and calculated IR spectra of the 1:1 complex in the near IR region[5] are reproduced in Fig. 5. It can be seen that transitions corresponding to free N1H and N7H stretching vibrations of UA are observed at 3449 and 3524 cm^{-1}, respectively, while those of free N3H and N9H stretches are absent in the spectrum. The finding firmly establishes that the latter two NH sites are occupied by H-bonding with MEL, which is consistent with a nonplanar pair, either structure 893 or 239 shown in Fig. 1. Unfortunately, the IR spectra calculated for the two structures shown in Fig. 5 are very similar each other, which makes unequivocal assignments of the experimental spectra difficult. It is also important to note that a broad absorption band is observed in the low-frequency region of 2500–2850 cm^{-1}. This large red-shift is explained to occur by the formation of a robust H-bond between hydrogen atom of the NH site (N3H or N9H) of UA and nitrogen atom of MEL ring (NH···N).[5] In both UA-MEL structures, the other two H-bonds, CO···HN(amino) and NH···N(amino), are calculated to be much weaker than the middle H-bond, as can be seen in Fig. 1.

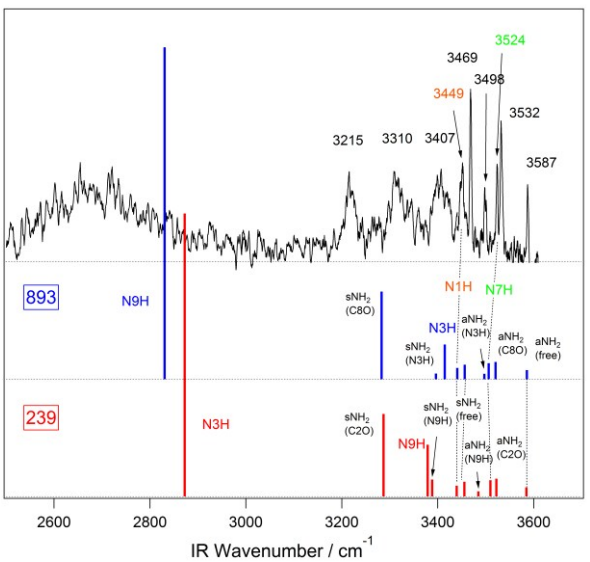

Fig. 5 Near-IR spectrum of the UA–MEL complex recorded between 2500 and 3650 cm^{-1} with the UV probe frequency at 34600 cm^{-1}. Vibrational spectra calculated for structures 893 and 239 (scaled by a factor of 0.955, see ref. 5) are shown in lower two panels. Assignments for the amino stretching vibrations of MEL are shown in black, and the corresponding H-bonding sites of UA are indicated in parentheses.

To distinguish between the two possible nonplanar structures of the UA–MEL complex, it is essential to examine their CO stretching vibrations. Fig. 6 shows the result of the mid-IR measurement together with the calculated and scaled stick spectra for the two structures. As described above, C8O

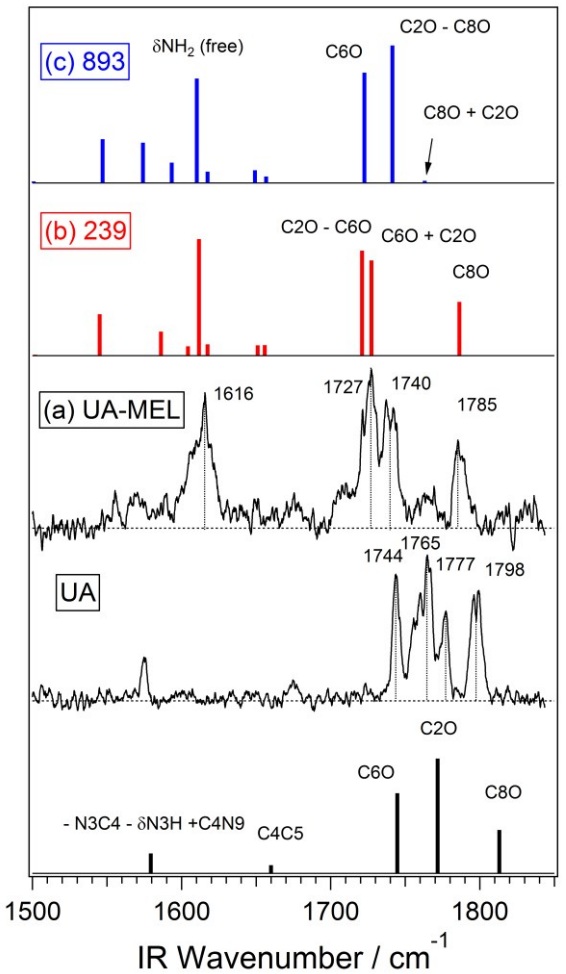

Fig. 6 (a) Mid-IR spectrum recorded for the UA–MEL complex with the UV probe frequency at 34600 cm^{-1}. Vibrational spectra calculated for structures 239 and 893 (scaled by a factor of 0.982) are shown in parts (b) and (c), respectively. The vertical lines in the experimental spectra correspond to positions of the indicated frequencies. The monomer spectra are shown in lower two panels for comparison.

stretching mode of monomer UA is mixed with C2O stretch mode, i.e., C8O ± C2O. In the case of the UA–MEL complex, this coupling may be lifted if the C2O site is H-bonded with MEL, quite similar to the monohydrate W23. Thus, the strong transition at 1785 cm^{-1} in the calculated spectrum of Fig. 6(b) is associated with pure C8O stretch mode of structure 239. In structure 893, mode coupling between the two stretches C8O and C2O is still effective and the IR intensity of their in-phase composition C8O + C2O is calculated to be remarkably weak as displayed in Fig. 6(c). This mode coupling behaviour is similar to the pattern observed for the corresponding two modes of the monohydrate W89 shown in Fig. 3(c). On this basis, the sharp transition observed at 1785 cm^{-1} is firmly assigned to pure C8O stretching vibration of structure 239, which supports the previous assignment made based on the near-IR spectrum in Fig. 5. The other two peaks at 1727 and 1740 cm^{-1} are assigned to mixed modes of C2O and C6O stretches. The intense peak appearing at 1616 cm^{-1} is due to bending vibration of the free amino group of MEL (δNH_2), which appears slightly higher in frequency than that measured in gas phase at 150°C (1598 cm^{-1}).[33] Vibrational assignments

for other peaks appearing in the calculated spectra, together with those of structure 678, are shown in Fig. S2 (ESI †).

The fact that the IR spectral pattern of the UA–MEL complex in Fig. 6(a) is nearly independent of the probe UV frequency at >34000 cm^{-1} suggests that a single structural isomer accounts for the observed UV spectrum To justify this conjecture, we have scanned the probe UV frequency with IR laser fixed to free C8O stretching peak at 1785 cm^{-1}. With this IR irradiation, only structure 239 will be depopulated while structure 893, if exists, survives. The resulting IR-depleted UV spectrum is shown in Fig. 7. It can be seen that the two spectra with IR laser turned on (I_{on}) and off (I_{off}), are very similar in the intensity distribution at >34000 cm^{-1}. Furthermore, the diffrence spectrum $I_{on} - I_{off}$ also resembles these two spectra. This finding seems to support the previous assignment that the UV spectrum consists only of structure 239 in this frequency region.

It should also be noted in Fig. 7 that the UV spectrum I_{off} reveals weak, gradually diminishing features that extend to

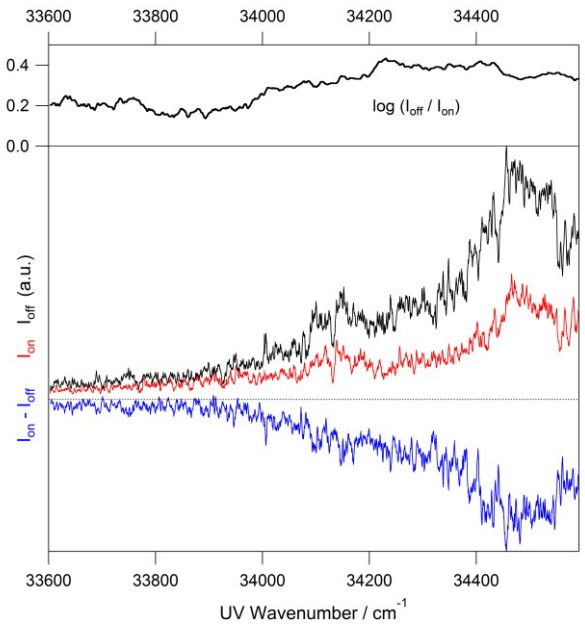

Fig. 7 UV spectra of the UA-MEL complex recorded with IR laser turned on at the 1785 cm^{-1} peak (I_{on}) and off (I_{off}), and their difference spectrum ($I_{on} - I_{off}$). Depletion yield derived from the relation log (I_{off} / I_{on}) plotted as a function of UV frequency is shown in top panel.

lower frequency region of 33600 cm^{-1}. However, IR–UV double resonance measurements in this UV probe region have failed due to its low intensity. Instead, we have examined the IR-depletion yield of UV signal, which is defined as log (I_{off} / I_{on}), as a function of the UV frequency. The resulting curve is shown in top panel of Fig. 7. It appears to vary less in the range above 34100 cm^{-1}, with values of about 0.4. This agrees qualitatively with the assignment that spectral features of other isomers having no free C8O group (e.g., structure 893) are not present in this region. It can also be seen that depletion yield decreases to approximately 0.2 in the range below 34000 cm^{-1}, possibly an indication of the existence of other structural isomers shown in Fig. 1. Since neither structure 893 nor 678 possesses free C8O group, they cannot be depleted with this IR irradiation, which are expected from the calculated frequencies shown in Fig. S2 (ESI †).

Conclusions

The IR spectra of the two most stable monohydrated clusters of UA have been recorded in the mid-IR region using the IR-UV double resonance scheme. Based on the CO stretching vibrational frequencies, the acceptor sites of H-bonding with water are unambiguously identified. In one isomer, C2O and N3H sites of UA are linked by water molecule (W23) while in the other, C8O and N9H sites are hydrated (W89). The normal mode analysis provided by DFT frequency calculation reveals that C8O and C2O stretch modes of the isomer W89 are strongly coupled as a result of hydration to the C8O site. Consequently, the IR intensity of their in-phase contribution appears to be significantly suppressed, in good agreement with the calculated spectra. In contrast, such mode coupling is nearly absent in isomer W23, thus giving rise to a strong absorption band corresponding to that of monomer.

For the 1:1 complex of UA and MEL, our previous study performed in the near-IR frequency region showed that the observed isomer corresponds to one of the two most stable structures (239 and 893), both having a triple H-bonded pair of nonplanar geometry. The observed mid-IR spectrum of this complex showed that its C8O stretch mode is not influenced by the complexation with MEL, which is consistent with the calculated lowest energy structure 239. To confirm the above structural assignments of the monohydrates and complex with MEL, IR depletion spectra have been recorded by scanning UV frequency while IR laser tuned to specific IR transitions of each isomer for depopulation.

The present results obtained for the monohydrate of UA and UA–MEL complex show that complexation with MEL occurs at the H-bonding sites of UA which are also used for hydration. Thus, we expect that once MEL occupies these H-bonding sites, UA is less likely to accommodate water molecules, an implication that formation of insoluble urinary stones is facilitated by the complexation. More importantly, it is found that vibrational motions of UA are significantly altered by hydration or complexation with MEL, depending on the H-bonding donor site. Such vibrational mode mixing in biomolecules, which is promoted by specific H-bonding, may have profound effects on the biological functions.

Acknowledgements

This work was supported by the Grant-in-Aid from JSPS (25410023). We thank Dr. H. Asami for computational assistance.

Notes and references

Graduate School for Bio- and Nanosystem Sciences, Yokohama City University, 22-2 Seto, Kanazawa-ku, Yokohama 236-0027, Japan. Fax: 81 45 787 2413; Tel: 81 45 787 2179; E-mail: saigusa@yokohama-cu.ac.jp
‡*Current address*: *Molecular Spectroscopy Laboratory, RIKEN, 2-1 Hirosawa, Wako 351-0198, Japan.*

† Electronic Supplementary Information (ESI) available: (i) Fig. S1 – Calculated IR spectra and vibrational assignments for the three lowest energy isomers of the monohydrated clusters of UA. (ii) Fig. S2 – Calculated IR spectra and vibrational assignments for the three lowest energy isomers of the UA–MEL complex. See DOI: 10.1039/b000000x/

1 G. A. Jeffery and W. Saenger, *Hydrogen Bonding in Biological Structures*; Springer-Verlag: Berlin, 1991.
2 M. S. de Vries and P. Hobza, *Annu. Rev. Phys. Chem.*, 2007, **58**, 585.
3 D. Voet, J. G. Voet and C. W. Pratt, *Fundamentals of Biochemistry: Life at the molecular level*, 4th edition; Wiley: New York, 2012, Ch. 23, pp. 814-816.
4 H. Asami, S. Urashima and H. Saigusa, *Phys. Chem. Chem. Phys.*, 2011, **13**, 20476.
5 H. Asami and H. Saigusa, *J. Phys. Chem. B*, 2014, **118**, 4851.
6 K. Sharma and M. Paradakar, *Food Sec.*, 2010, **2**, 97.
7 C. G. Skinner, J. D. Thomas and J. D.Osterloh, *J. Med. Toxicol.*, 2010, **6**, 50.
8 R. Reimschuessel and B. Puschner, *J. Med. Toxicol*., 2010, **6**, 468.
9 Q. Sun, Y. Shen, N. Sun, G. Zhang, Z. Chen, J. Fang, L. Jia, H. Xiao, X, Li and B. Puschner, *Eur. J. Pediatr.*, 2010, **169**, 483.
10 X. Cong, X. Sun and B. Ning, *J. Clin. Lab. Anal.*, 2013, **27**, 59.
11. M. Gerhards, C. Unterberg and A. Gerlach, *Phys. Chem. Chem. Phys.*, 2002, **4**, 5563.
12. H. Fricke, A. Gerlach and M. Gerhards, *Phys. Chem. Chem. Phys.*, 2006, **8**, 1660.
13. M. Miyazaki, J. Saikawa, H. Ishizuki, T. Taira and M. Fujii, *Phys. Chem. Chem. Phys.*, 2009, **11**, 6098.
14 J. M. Bakker, L. M. Aleese, G. Meijer and G. von Helden, *Phys. Rev. Lett.*, 2003, **91**, 203003
15 J. M. Bakker, I. Compagnon, G. Meijer, G. von Helden, M. Kabeláč, P. Hobza and M. S. de Vries, *Phys. Chem. Chem. Phys.*, 2004, **6**, 2810.
16 A. Golan, N. Mayorkas, S. Rosenwaks and I. Bar, *J. Chem. Phys.*, 2009, **131**, 024305.
17 N. Mayorkas, I. Malka and I. Bar, *Phys. Chem. Chem. Phys.*, 2011, **13**, 6808.
18 N. Mayorkas, S. Izbitski, A. Bernat and I. Bar, *J. Phys. Chem. Lett.*, 2012, **3**, 603.
19 P. Zielke and M. A. Suhm, *Phys. Chem. Chem. Phys.*, 2007, **9**, 4528.
20 T. N. Wassermann and M. A. Suhm, *J. Phys. Chem. A*, 2010, **114**, 8223.
21 H. Saigusa, A. Tomioka, T. Katayama and E. Iwase, *Chem. Phys. Lett.*, 2006, **418**, 119.
22 H. Saigusa, S. Urashima and H. Asami, *J. Phys. Chem. A*, 2009, **113**, 3455.
23 H. Asami, S. Urashima and H. Saigusa, *Phys. Chem. Chem. Phys.*, 2009**, 11**, 10466.
24 S. Urashima, H. Asami, M. Ohba and H. Saigusa, *J. Phys. Chem. A*, 2010, **114**, 11231.
25 H. H. Nielsen, *Phys. Rev.*, 1941, **59**, 565.
26 M. Mons, I. Dimicoli, F. Piuzzi, B. Tardivel and M. Elhanine, *J. Phys. Chem. A*, 2002, **106**, 5088.
27 24 M. J. Frisch, G. W. Trucks, H. B. Schlegel, G. E. Scuseria, M. A. Robb, J. R. Cheeseman, G. Scalmani, V. Barone, B. Mennucci, G. A. Petersson, H. Nakatsuji, M. Caricato, X. Li, H. P. Hratchian, A. F. Izmaylov, J. Bloino, G. Zheng, J. L. Sonnenberg, M. Hada, M. Ehara, K. Toyota, R. Fukuda, J. Hasegawa, M. Ishida, T. Nakajima, Y. Honda, O. Kitao, H. Nakai, T. Vreven, J. A. Montgomery Jr., J. E. Peralta, F. Ogliaro, M. Bearpark, J. J. Heyd, E. Brothers, K. N. Kudin, V. N. Staroverov, R. Kobayashi, J. Normand, K. Raghavachari, A. Rendell, J. C. Burant, S. S. Iyengar, J. Tomasi, M. Cossi, N. Rega, J. M. Millam, M. Klene, J. E. Knox, J. B. Cross, V. Bakken, C. Adamo, J. Jaramillo, R. Gomperts, R. E. Stratmann, O. Yazyev, A. J. Austin, R. Cammi, C. Pomelli, J. W. Ochterski, R. L. Martin, K. Morokuma, V. G. Zakrzewski, G. A. Voth, P. Salvador, J. J. Dannenberg, S. Dapprich, A. D. Daniels, O. Farkas, J. B. Foresman, J. V. Ortiz, J. Cioslowski and D. J. Fox, Gaussian 09 Revision A.02, Gaussian, Inc., Wallingford, CT, 2009.
28 A. K. Chandra and Th. Zeegers-Huyskens, *J. Mol. Struct. (THEOCHEM)*, 2007, **811**, 215.
29 S. Yamazaki, S. Urashima, H. Saigusa and T. Taketsugu, *J. Phys. Chem. A*, 2014, **118**, 1132.
30 K. M. Anderson, G. M. Day, N. J. Paterson, P. Byrne, N. Clarke and J. W. Steed, *Angew. Chem. Int. Ed.*, 2008, **47**, 1058.
31 P. Pulay, G. Fogarasi, F. Pang and J. E. Boggs, *J. Am. Chem. Soc.*, 1979, **101**, 2550.
32 M. Majoube and G. Vergoten, *J. Mol. Struct.*, 1993, **294**, 41.
33 Y. Wang, A. M. Mebel, C. Wu, Y. Chen, C. Lin and J. Jiang, *J. Chem. Soc., Faraday Trans.*, 1997, **93**, 3445.